ACS APPLIED MATERIALS & INTERFACES

Research Article

Cite This: ACS Appl. Mater. Interfaces XXXX, XXX, XXX−XXX

www.acsami.org

Electrochemical Biosensor for DNA Methylation Detection through Hybridization Chain-Amplified Reaction Coupled with a Tetrahedral DNA Nanostructure

Xi Chen,[†,§,⊥,▽] Jian Huang,[∥,§] Shu Zhang,[⊥,†,§] Fei Mo,[⊥,†] Shasha Su,[†] Yan Li,[§] Lichao Fang,[§] Jun Deng,[§] Hui Huang,[§] Zhaoxun Luo,[*,#,‡] and Junsong Zheng[*,§]

[†]Department of Basic Clinical Laboratory Medicine, School of Clinical Laboratory Science and [‡]School of Pediatrics, Guizhou Medical University, No. 9 Beijing Road, Yunyan District, Guiyang 550004, China

[§]Department of Clinical and Military Laboratory Medicine, College of Medical Laboratory Science, Army Medical University, 30 Gaotanyan Street, Shapingba District, Chongqing 400038, China

[∥]Department of Biochemistry, [⊥]Department of Clinical Laboratory, and [#]Guizhou Children's Medical Center, Affiliated Hospital of Guizhou Medical University, Guiyang 550004, China

Supporting Information

ABSTRACT: DNA methylation is a key factor in the pathogenesis of gene expression diseases or malignancies. Thus, it has become a significant biomarker for the diagnosis and prognosis of these diseases. In this paper, we designed an ultrasensitive and specific electrochemical biosensor for DNA methylation detection. The platform consisted of stem−loop−tetrahedron composite DNA probes anchoring at a Au nanoparticle-coated gold electrode, a restriction enzyme digestion of *Hpa*II, and signal amplification procedures including electrodeposition of Au nanoparticles, hybridization chain reaction, and horseradish peroxidase enzymatic catalysis. Under optimal conditions, the design showed a broad dynamic range from 1 aM to 1 pM and a detection limit of about 0.93 aM. The approach also showed ideal specificity, repeatability, and stability. The recovery test demonstrated that the design is a promising platform for DNA methylation detection under clinical circumstances and could meet the need for cancer diagnosis.

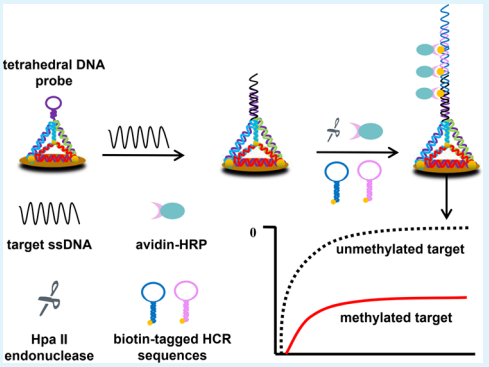

KEYWORDS: *DNA methylation, hybridization chain reaction, biosensor, DNA tetrahedral nanostructure probe, multiple signal amplification*

INTRODUCTION

DNA methylation, in which the 5-methylcytosine (5-mC) is catalyzed by the DNA methyltransferase, is confirmed to be a key factor in mammalian development and the silencing of gene expression, and many studies have verified that DNA methylation is relevant to the pathogenesis of many diseases, such as diabetes, genetic diseases, and malignancies; therefore, the identification of DNA methylation has great significance for the prediction and prognosis of these diseases.[1−7] In the past decades, numerous approaches have been widely used for the identification of DNA methylation, such as sequencing analysis, methylation-specific polymerase chain reaction, high-performance liquid chromatography, etc.[8−11] These conventional methods generally demand costly instruments or intricate analysis procedures, and therefore, establishing a fast, precise, stable, low-cost method to analyze the methylation in CpG dinucleotides is necessary; however, electrochemical biosensing strategies have the above-mentioned advantages and a high sensitivity with a low detection limit.[12,13] Furthermore, owing to its ability to achieve multitarget analysis,[14] the development of electrochemical biosensing detection of epigenetic factors has successfully attracted considerable attention from researchers.

Based on the Watson−Crick complementary base-pairing theory, the construction of the capture probe is vital for the specificity and sensitivity of electrochemical DNA biosensors (E-DNA sensor). Thiolated single-stranded DNA (ssDNA) probes are commonly used as the recognition element as they do not contain secondary structures and can readily self-assemble on gold surfaces.[15] However, the density and orientation of ssDNA probes are not easy to control, which have strong impacts on the hybridization efficiency between the capture probes and the target sequences.[16] Recent studies show that the tetrahedral DNA nanostructure probe (TSP) is becoming the mainstream of capture probe construction in E-DNA sensors.[17−19] TSP, shaped like a pyramid scaffold, is synthesized from three thiolated DNA sequences and one probe-containing

Received: November 16, 2018
Accepted: January 9, 2019
Published: January 9, 2019

DOI: 10.1021/acsami.8b20144
ACS Appl. Mater. Interfaces XXXX, XXX, XXX−XXX

Scheme 1. Schematic Illustration of the Multiple Signal Amplification Biosensing Detection for DNA Methylation

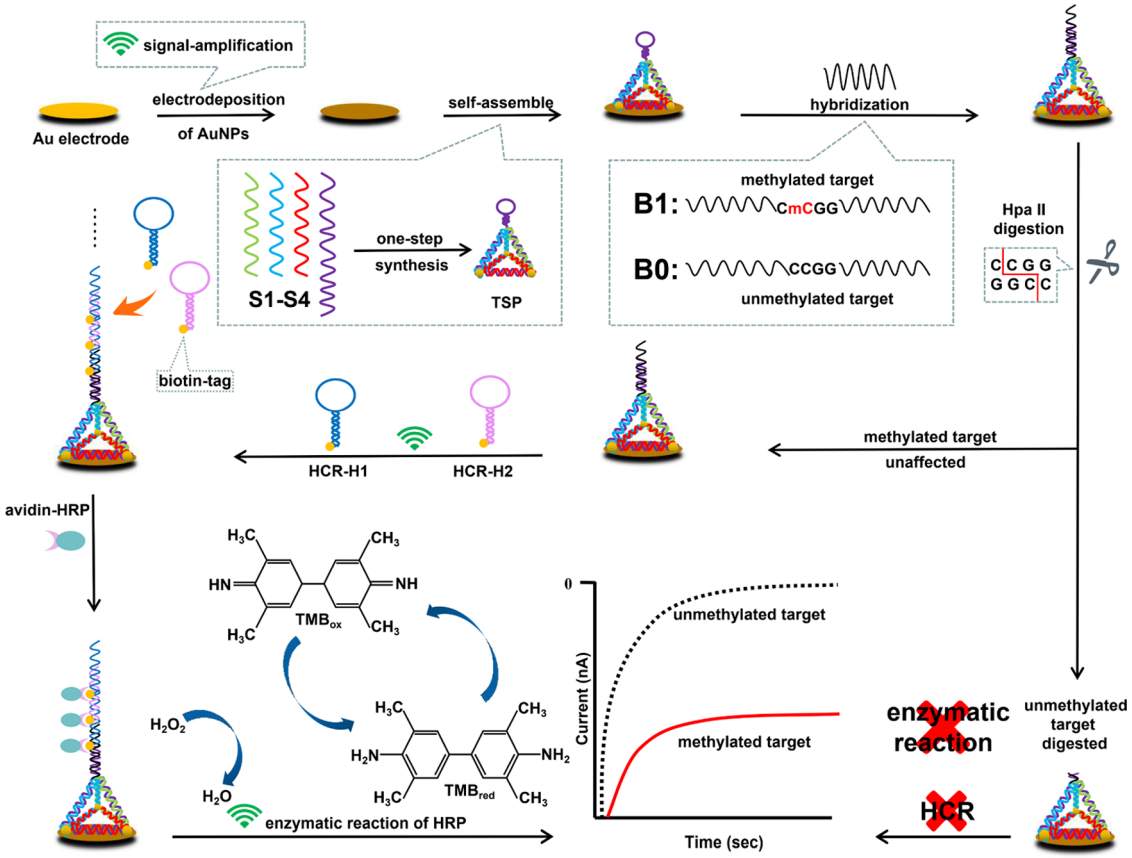

DNA sequence.[15,20] Compared with the conventional ssDNA probe, TSP is superior in the following aspects: the three thiolated sequences can achieve the TSP anchoring more easily at the electrode surface and greatly enhance its stability; the scaffold of TSP can enlarge the probe-to-probe space, which can facilitate the orientation and density of capture probes, thus avoiding interprobe entanglement; moreover, TSP modification has an excellent passivation effect on the electrode surface, which can prevent the nonspecific adsorption of small molecules.[15,19,21,22]

However, basic E-DNA sensors may not be able to detect the target sequences of trace concentrations or within complex components; therefore, signal amplification procedures are extensively used in establishing biosensing strategies. Nanomaterials such as metallic nanoparticles, multiwall carbon nanotubes, magnetic beads, or reduced graphene oxide are widely used.[23−26] Enzymatic amplification is also widely used in fabricating biosensors.[17,27] Horseradish peroxidase (HRP) is one of the most popular redox enzymes for its stability, efficiency, and relatively low cost.[17] After conjugating with the probe−target complex through covalent interactions such as biotin−avidin or antigen−antibody immunoreaction, the HRP can anchor at the surface of the working electrode, and thus, it could catalyze the redox reactions and amplify the electrochemical signal.[15,28] In addition, since the target molecules of the E-DNA sensor are nucleic acids of specific sequences, in vitro nucleic acid amplification techniques can be employed in the E-DNA sensor as well, such as the hybridization chain reaction (HCR), ligase chain reaction, etc.[29−31]

The DNA methylation biosensing platform is established by combining the E-DNA biosensor with certain methylation-specific analytical methodologies. For now, these methods generally fall into three main categories: restriction endonuclease-based, immunoreaction-based, and bisulfite conversion-based.[32] Bisulfite conversion is a classical and popular method for DNA methylation detection and many DNA methylation biosensors are established based on it.[33−35] However, the bisulfite conversion process may lead to a low conversion efficiency, false results, a longer assay time, and irreversible changes of the target sequence,[6] which can lead to the loss of targets;[32,36] therefore, the other two types are more commonly used. By employing methylation-specific antibodies, the immunosensor could accomplish DNA methylation measurement.[26,28,37] Methylation-specific restriction endonucleases, such as the *Dpn*I or *Hpa*II, can cleave unmethylated DNA only,[25,38,39] and thus, a distinguishable electrochemical signal between unmethylated and methylated DNA sequences can be obtained.

Herein, we propose an ultrasensitive electrochemical biosensor for DNA methylation detection (Scheme 1). A Au nanoparticle (AuNP)-coated gold disk electrode was modified with TSP, whereas the linear ssDNA capture probe at the vertice of the TSP was replaced with a stem−loop capture probe.[40] The stem−loop capture probe could enhance the specificity of the biosensor,[41] leading to an ideal signal-to-noise ratio in biosensing strategies. After hybridizing with the target sequence, which had a palindrome sequence of 5′-C-C-G-G-3′, the digestion procedure of *Hpa*II was carried out. The digestion was blocked when the target sequence was methylated or else the unmethylated target was digested and rinsed away.[38,42] Then, the HCR and HRP amplifications were performed, and finally, a distinguishable signal could be attained, representing

DOI: 10.1021/acsami.8b20144
ACS Appl. Mater. Interfaces XXXX, XXX, XXX−XXX

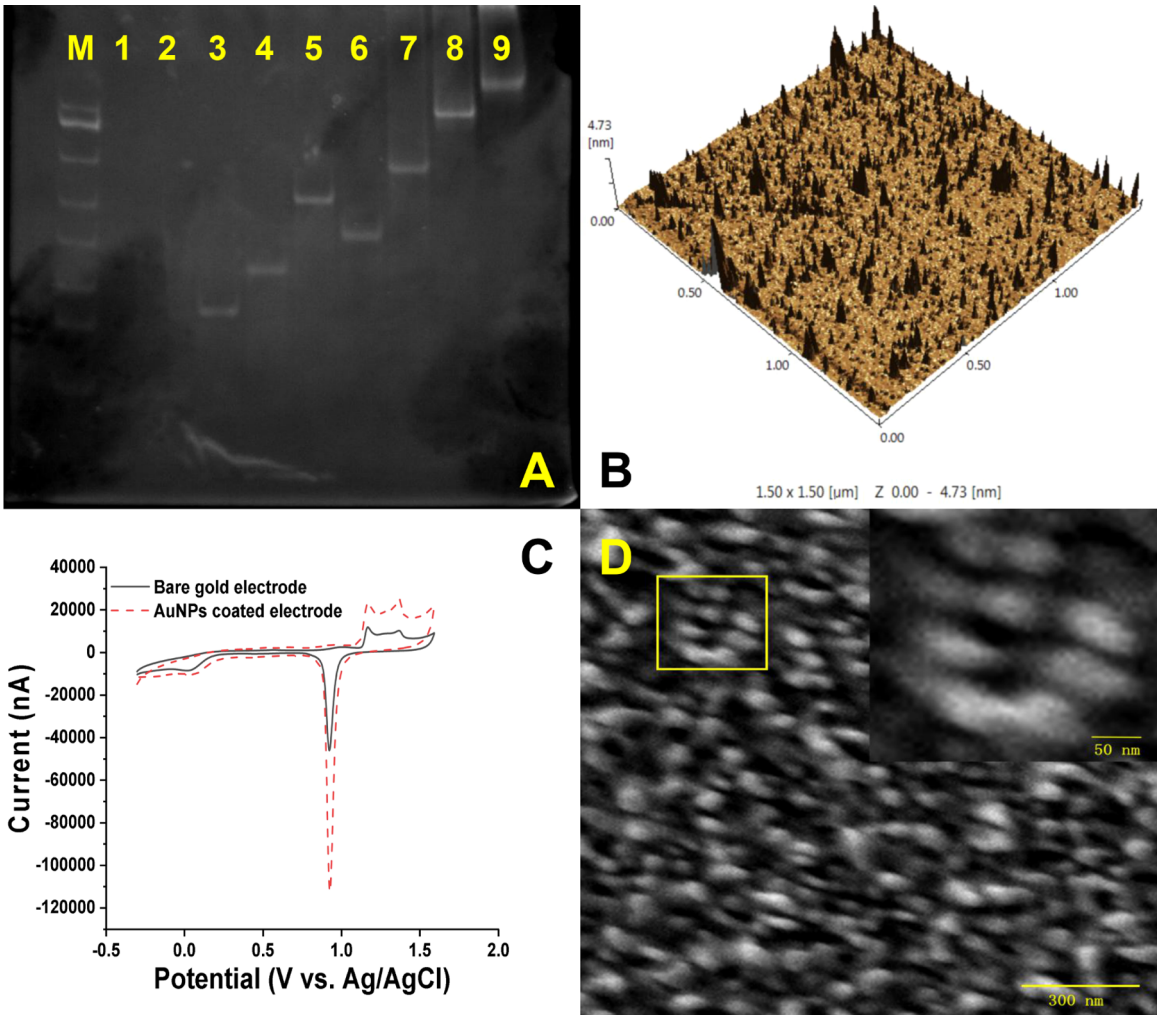

Figure 1. (A) PAGE image of TSP: lane M, 25 bp ladder; lane 1, S1; lane 2, S3; lane 3, S4; lane 4, S1 + S2; lane 5, S1 + S4; lane 6, S2 + S3; lane 7, S1 + S2 + S3; lane 8, S2 + S3 + S4; lane 9, S1 + S2 + S3 + S4. (B) AFM imaging of TSP on freshly cleaved mica. (C) Cyclic voltammograms (CV) of the bare gold electrode (solid) and the AuNP-coated gold electrode (dash) in 0.5 M H_2SO_4 (scan rate: 50 mV/s). (D) Scanning electron microscopy (SEM) image of the AuNP-coated gold electrode; scale bar: 300 nm. Inset shows the enlarged image of the yellow frame area; scale bar: 50 nm.

the different methylation status of the target sequences. In summary, due to the multiple signal amplification procedures and methylation-sensitive restriction enzyme treatment, this approach could be a reliable solution for the measurement of DNA methylation.

EXPERIMENTAL SECTION

Materials and Reagents. All DNA sequences were synthesized and purified by Shanghai Sangon Biotechnology (Shanghai, China). The base sequences of the oligonucleotides are shown in Table S1, and the recognition sites for *Hpa*II endonuclease are presented in bold italic type. Phosphate buffered saline (PBS, pH 7.2−7.4) and Tris−ethylenediaminetetraacetic acid buffer (TE, pH 8.0) were purchased from Beijing Dingguo Changsheng Biotechnology (Beijing, China). The tetramethylbenzidine (TMB) substrate (enhanced K-Blue, in the format of a ready-to-use reagent with long-term stability, H_2O_2 included) was supplied by Neogen (Lexington, KY). Streptavidin−horseradish peroxidase (S−HRP) was purchased from Sigma-Aldrich (St. Louis). Restriction endonuclease *Hpa*II and CutSmart buffer were supplied by New England Biolabs (Ipswich, MA). Bovine serum albumin (BSA) was purchased from Genview (Beijing, China). $HAuCl_4 \cdot 3H_2O$ was purchased from J&K Chemical (Beijing, China). Tris(2-carboxyethyl)phosphine (TCEP) was purchased from Shanghai Sangon Biotechnology (Shanghai, China). All chemicals were used without further purification. Other reagents were of analytical reagent grade and purchased from Sinopharm Chemical Reagent (Shanghai, China). All of the aqueous solutions were prepared with ultrapure water (18.2 MΩ cm resistivity) from a Huachuang DLH1-40L-D system (Chongqing, China).

The apparatus involved in this study is given in the Supporting Information.

Synthesis of the DNA Tetrahedral Nanostructure Probe. The four tetrahedral nanostructured probe oligonucleotides (S1−S4) were dissolved in TE buffer to obtain the 50 μM stock solutions (stored at −20 °C). Each oligonucleotide (1 μL) was added to a centrifuge tube coupled with 41 μL of TM buffer (20 mM Tris and 50 mM $MgCl_2$, pH 8.0) and 5 μL of TCEP solution (30 mM TCEP in ultrapure water). The DNA probe mixture was then heated to 95 °C for 2 min and cooled to 4 °C over 30 s; afterward, the 1 μM TSP working solution was successfully synthesized.[19]

Biosensing Interface Fabrication. The 2 mm-diameter polycrystalline gold electrode was polished with 0.5 and 0.05 μm alumina slurry, respectively, on chamois leather, and then sonicated in ultrapure water, ethanol, and ultrapure water for 5 min successively. After dipping in Piranha solution (98% H_2SO_4 and 30% H_2O_2, v/v = 3:1; **Caution:** this solution is highly corrosive and the mixing process is extremely exothermic; great care should be taken) for over 15 min, electrochemical cleansing of the electrode was carried out in 0.5 M H_2SO_4 until a reduplicative curve was achieved. Thus, the bare gold electrode was completely cleansed and could be used for the electrodeposition of

DOI: 10.1021/acsami.8b20144
ACS Appl. Mater. Interfaces XXXX, XXX, XXX−XXX

AuNPs. The electrodeposition was carried out by immersing the electrode into $HAuCl_4$ solution (10 mM $HAuCl_4$ and 0.5 M H_2SO_4 in ultrapure water) to get a larger specific surface area. Afterward, 4 μL of freshly synthesized TSP working solution was pipetted on the surface of the AuNP-coated gold electrode. The electrode was then capped with a plastic cap to prevent the solution from drying out and incubated at room temperature for 3 h. This step was followed by rinsing thoroughly with 1× PBS and ultrapure water, respectively, to remove the nonspecific adsorbed TSP.

Hybridization with the Target and Enzymatic Digestion. Ten microliters of the target sequence (concentration ranging from attomolar to nanomolar) in hybridization buffer (20 mM $MgCl_2$ and 1 M NaCl in 10× PB, pH 7.4) were pipetted on the surface of the electrode and incubated at 37 °C for 1 h. After rinsing thoroughly with 1× PBS and ultrapure water, methylation-specific digestion was performed in 1× CutSmart buffer (50 mM KAc, 20 mM Tris−Ac, 10 mM $Mg(Ac)_2$, 100 μg/mL BSA, pH 7.9) containing 50 U/mL *Hpa*II at 37 °C for 2 h. Thereafter, the electrode was again rinsed thoroughly with 1× PBS and ultrapure water, respectively.

Signal Amplification and Electrochemical Detection. Prior to the HCR, 1 μM H1 and H2 (in TE buffer) were heated separately to 95 °C for 5 min and cooled on ice for 15 min subsequently, and then mixed together in 1× SPSC buffer (1 M NaCl, 50 mM NaH_2PO_4, pH 7.5) to get a concentration of 0.1 μM before use. The HCR was carried out by pipetting 15 μL of the H1/H2 mixture on the electrode surface and incubating at 37 °C for 2 h. After rinsing thoroughly with 1× PBS and ultrapure water, respectively, the 0.01 mg/mL S−HRP solution (1× PBS with 1% BSA and 0.5% casein) was pipetted to the electrode surface and incubated for 15 min at room temperature. The electrode was rinsed with 1× PBS and ultrapure water, respectively, and then it was ready for the electrochemical measurements in TMB solution.

RESULTS AND DISCUSSION

Characterization of TSP. The TSP was synthesized from four oligonucleotides S1−S4 and then analyzed by 10% polyacrylamide gel electrophoresis (PAGE). We employed different combinations of the four oligonucleotides to prove the successful formation of the TSP products. Figure 1A demonstrates that the successfully synthesized TSP was moving significantly slower than any other combinations due to its complex three-dimensional structure.[19,43] We also employed atomic force microscopy (AFM) to characterize TSP by pipetting it on a freshly cleaved mica chip. The image (Figure 1B) illustrates that the height of the successfully fabricated TSP is about 4.73 nm, which is close to the theoretical value (4.72 nm).

Characterization of the Electrochemical Biosensor. AuNPs are widely used to enlarge the electroactive surface area and facilitate the electron mobility of electrochemical biosensors.[13,44] The cyclic voltammograms (CV) of the bare gold electrode and the AuNP-coated gold electrode in 0.5 M H_2SO_4 can be observed in Figure 1C. After electrodeposition of AuNPs, the reduction peak at about +930 mV was significantly increased, indicating that a larger electroactive surface area was obtained. According to the Randles−Sevcik equation, the electroactive area of the AuNP-coated gold electrode is 2.423 times larger than that of the bare gold electrode.

The SEM image of the AuNP-coated gold electrode is depicted in Figure 1D. According to the image, the average size of AuNPs is about 40 nm, demonstrating that a larger superficial area of the electrode was obtained via the electrodeposition of AuNPs.

Optimization of the Experimental Conditions. To achieve the optimal performance of the designed biosensor, the experimental conditions were optimized. As shown in Figure 2A, the incubation time of TSP is investigated in the range from

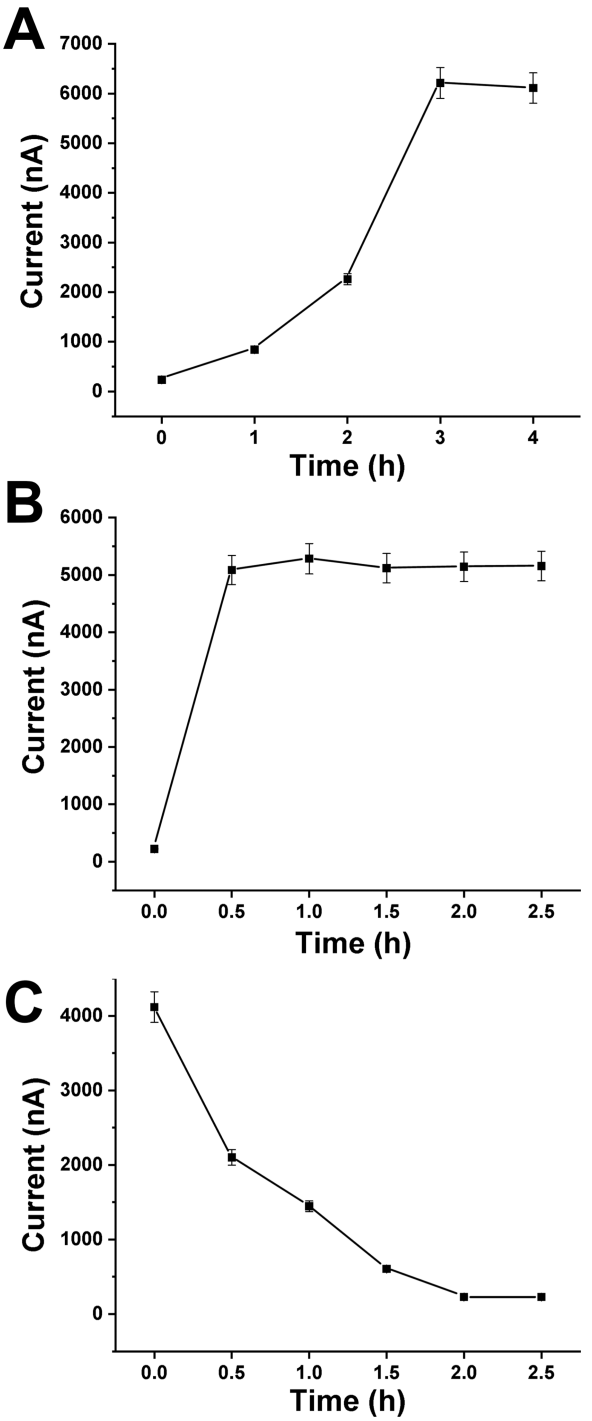

Figure 2. Chronoamperometric response signals of different experimental conditions: (A) incubation time of TSP, (B) hybridization time with the target, and (C) digestion time of *Hpa*II endonuclease. The error bars were obtained from three or more replicate tests.

0 to 4 h using 1 nM target with chronoamperometry. The incubation time was related to the density of anchored TSP, which could influence the hybridization efficiency with the target sequences. The response signal increased monotonically along with increasing time and reached the equilibrium status at 3 h; therefore, 3 h was chosen for the biosensor for further experiments. Besides, the core mechanism of the E-DNA biosensing detection was based on nucleic acid hybridization; therefore, we further explored the duration of the hybridization

DOI: 10.1021/acsami.8b20144
ACS Appl. Mater. Interfaces XXXX, XXX, XXX−XXX

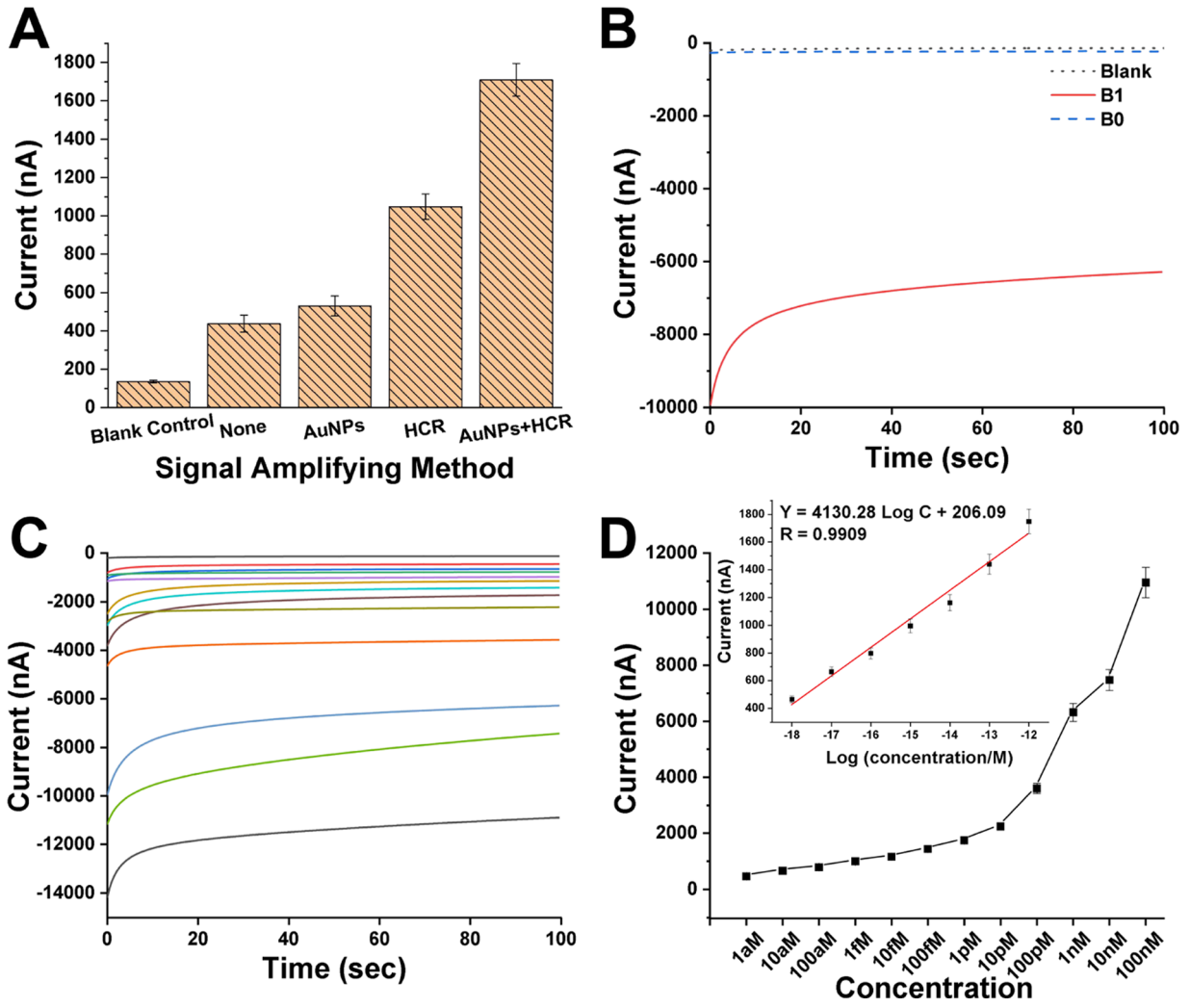

Figure 3. (A) Validation test of the signal amplification function. (B) Chronoamperometric response signals of the blank control (dot), unmethylated target (dash), and methylated target (solid). (C) Chronoamperometric response signals of 0 aM, 1 aM, 10 aM, 100 aM, 1 fM, 10 fM, 100 fM, 1 pM, 10 pM, 100 pM, 1 nM, 10 nM, and 100 nM methylated targets (from top to bottom). The initial potential was 100 mV (vs Ag/AgCl) and the runtime was 100 s. (D) The dose−response curve of different target concentrations. Inset shows the linear relationship between the chronoamperometric signals and the logarithm of target concentrations from 1 aM to 1 pM. The *y* and *x* axes represent the chronoamperometric response signal and the logarithm of concentrations of the target, respectively, and *R* stands for the correlation coefficient. The error bars were obtained from three or more replicate tests.

Table 1. Comparison with Previous Biosensing Studies on DNA Methylation[a]

no.	detection strategy	linear range (M)	limit of detection (M)	stability	repeatability (%)	references
1	photoelectrochemistry	1×10^{-13} to 1×10^{-9}	3.5×10^{-14}	90.28% in 28 days	6.89−7.57	45
2	DPV	1×10^{-15} to 1×10^{-9}	1×10^{-16}	92.9% in 30 days	6.6−9.1	46
3	DPV	1×10^{-13} to 5×10^{-9}	2×10^{-15}	stable in 8 weeks	2.4−6.3	47
4	DPV	5×10^{-7} to 2.3×10^{-3}	6×10^{-7}	93.8−95.9% in 4 weeks	2.9−4.9	48
5	amperometry	3.9×10^{-12} to 5×10^{-10}	3×10^{-17}	stable in 35 days	3.3	25
6	amperometry	8.7×10^{-11} to 2.5×10^{-9}	2.6×10^{-11}	no significant decrease during at least 35 days	4.3	28
7	amperometry	4.0×10^{-12} to 2.5×10^{-10}	1.2×10^{-12}		2.8	26
8	chronoamperometry	1×10^{-18} to 1×10^{-11}	9.326×10^{-19}	91.97% in 30 days	4.846	this work

[a]DPV—differential pulse voltammetry.

process. As shown in Figure 2B, in the time span from 0 to 2.5 h, the response signal increases at the outset and reached a climax at the time of 1 h; hence we chose 1 h as the time of hybridization. The digestion process of methylation-specific restriction endonucleases was crucial in this approach, and so we tested different digestion times as well. As shown in Figure 2C, the digestion time of *Hpa*II spans from 0 to 2.5 h. The digestion process toward unmethylated target sequences was almost completed at 2 h as its current signal was approximately equal to that of the blank control; hence, 2 h was chosen as the digestion time.

Performance of the Electrochemical Biosensor in DNA Methylation Detection. Cyclic voltammetry and chronoamperometry were used to characterize the process of DNA

DOI: 10.1021/acsami.8b20144
ACS Appl. Mater. Interfaces XXXX, XXX, XXX−XXX

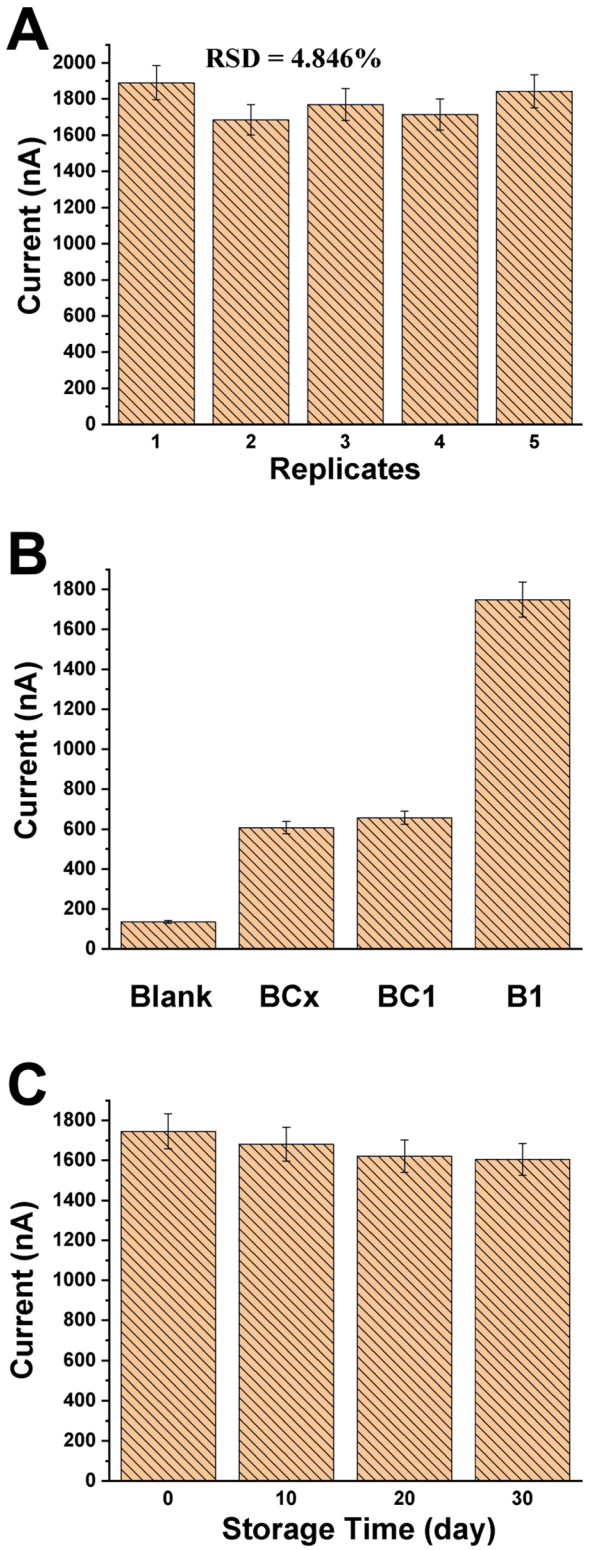

Figure 4. (A) Chronoamperometric response signals of repeat experiments. (B) Specificity of the biosensor in the detection of various DNA targets at 1 pM: completely matched target DNA (B1), single-base mismatched DNA (BC1), and multibase mismatched DNA (BCx). (C) Chronoamperometric response signals after 0−30 days of storage at 4 °C.

methylation detection. Figure S1 shows the cyclic voltammograms of the biosensor in the TMB substrate. In the blank control, two pairs of redox peaks demonstrate the redox reactions of TMB without HRP catalysis.[17] In the presence of target sequences, the conjugated HRPs were brought into the solution and increased the asymmetric redox peaks at +240 mV. This evidence illustrated the effective electrocatalysis of HRP and the successful detection of the target sequences.

Table 2. Experimental Results of the Recovery Test in Human Serum (n = 3)

sample	spiked (fM)	found (fM)	recovery (%)	RSD (%)
1	1	1.054	105.43	4.42
2	10	10.31	103.13	1.22
3	20	19.20	96.02	6.74
4	50	50.26	100.52	3.44
5	100	96.88	96.88	4.82

To validate the signal amplification behaviors of the designed biosensor, we investigated and compared the signal enhancement by the AuNPs and the HCR; four groups (1, no amplification; 2, only AuNPs; 3, only HCR; and 4, AuNPs + HCR) were set up to be detected with 1 pM methylated target. As shown in Figure 3A, the chronoamperometric signals of the four groups were about 437.9, 529.8, 1048, and 1709 nA, respectively. The chronoamperometric signal of group 4 was about 3.9, 3.22, and 1.63 times larger than those of groups 1, 2, and 3, respectively, indicating that the established signal amplification method was highly effective.

Figure 3B shows the different chronoamperometric signals of the methylated target (B1) and the unmethylated target (B0) with the concentration of 1 nM. The results demonstrate that the fabrication of our biosensor was achieved and the signal-to-noise ratio was acceptable. Methylated and unmethylated targets could be discriminated due to the catalysis of *Hpa*II. The unmethylated target was digested effectively and could not initiate the HCR or conjugate the S−HRP, leading to a signal (about 228.2 nA) approximately equal to that the blank control (about 135.6 nA). Conversely, *Hpa*II could not digest the recognition site 5′-C-mC-G-G-3′ in a methylated target; thus, the sticky end of the methylated target could initiate HCR and further conjugate numerous S−HRP via the biotin tags of H1 and H2 sequences, resulting in a strong chronoamperometric response signal (about 6315 nA) in the TMB substrate.

We also achieved quantitative measurement of methylated targets with concentrations ranging from 1 aM to 100 nM (Figure 3C). Impressively, the current of the 1 aM methylated target reached 464.4 nA, which was three times larger than that of the blank control. This indicated that the multiple signal amplification procedures in our biosensor operated effectively and could amplify the signal of the target with trace concentrations. Figure 3D displays the relationship between the chronoamperometric response signals and the target concentrations. The targets of various concentrations were effectively discriminated and the chronoamperometric signals increased monotonically with the rise of the target concentrations. The inset of Figure 3D shows the linear relationship between the chronoamperometric signals and the logarithm of target concentrations from 1 aM to 1 pM, which spans 7 orders of magnitude. The regression equation can be expressed as $Y = 4130.28 \log C + 206.09$ and the detection limit was about 0.93 aM. Both the low detection limit and the board dynamic range suggested that the ultrasensitive biosensor could be used to detect DNA methylation. The comparison with previous studies on DNA methylation (Table 1) also suggests that our design is a reliable approach for DNA methylation detection.

DOI: 10.1021/acsami.8b20144
ACS Appl. Mater. Interfaces XXXX, XXX, XXX−XXX

Repeatability, Specificity, and Storage Stability of the Electrochemical Biosensor. The repeat experiments were carried out by measuring 1 pM methylated target sequence (B1) five times under the same conditions. The relative standard deviation (RSD) was about 4.846%, suggesting a practicable repeatability of the biosensing strategy (Figure 4A).

The specificity experiments were conducted via a set of measurements of mismatched target sequences. The mismatched target sequences included a single-base and a multibase mismatched methylated DNA. The measurements were performed with 1 pM targets of each type under the same conditions. As the results revealed (Figure 4B), facilitated by the TSP and stem−loop capture probes, the biosensor succeeded in discriminating even a single-base mismatch in DNA sequences, demonstrating that the biosensor was of high specificity.

The storage stability was also investigated by preparing and storing the electrode under the same conditions. The electrodes were stored at 4 °C, capped with plastic caps, and detected every 10 days. As Figure 4C shows, the response signals decrease gradually with the storage time extending from 0 to 30 days. The biosensor lost about 8.03% of its initial response signal, suggesting the acceptable stability of this platform.

Recovery Test of the Prepared Biosensor. To validate the performance of the designed approach for DNA methylation detection in endogenous biological samples, which is significant for clinical application, we conducted a series of recovery tests. Human serum from a healthy volunteer served as the complex biological system. A certain amount of methylated DNA (B1) was spiked into the serum and detected undiluted. Table 2 shows the results of the recovery test: the percentage recoveries of the added DNA varied from 96.02 to 105.43%, with the RSD ranging from 1.22 to 6.74%, suggesting that the proposed biosensor is highly resistant to biological interference and effective toward real sample measurement.

CONCLUSIONS

In this paper, an ultrasensitive and specific electrochemical biosensor for the detection of DNA methylation was successfully fabricated. Under the optimal experimental conditions, the design showed a broad dynamic range from 1 aM to 1 pM and a detection limit lower than 1 aM. The specificity, stability, and repeatability were also successfully verified. According to the results, our design was much more sensitive in the measurement of DNA methylation compared with other approaches due to the employment of TSP and HCR, demonstrating that the design is a reliable electrochemical biosensing method for DNA methylation detection and could meet the need for cancer diagnosis at an early stage with trace methylated DNA concentrations.

ASSOCIATED CONTENT

Supporting Information

The Supporting Information is available free of charge on the ACS Publications website at DOI: 10.1021/acsami.8b20144.

Apparatus used for all experiments, cyclic voltammograms of the biosensor in TMB solution (Figure S1), and oligonucleotide sequences of the target DNA, probes, single-base and multibase mismatched DNA and all other DNA sequences used in this study (Table S1) (PDF)

AUTHOR INFORMATION

Corresponding Authors

*E-mail: luozhaoxun@gmc.edu.cn. Tel: +86 851 86761424 (Z.L.).

*E-mail: zhengalpha@sina.com. Tel: +86 23 68771651 (J.Z.).

ORCID

Junsong Zheng: 0000-0002-5248-4209

Notes

The authors declare no competing financial interest.

▽X.C.: Combined training postgraduate of the Army Medical University and Guizhou Medical University.

ACKNOWLEDGMENTS

We appreciate the financial support by the National Natural Science Foundation of China (Nos. 81572078, 81401722, and 81873982) and the Third Military Medical University Medical Creative Research Foundation (SWH2016JCYB-62 and SWH2016JCYB-33).

REFERENCES

(1) Ellis, L.; Atadja, P. W.; Johnstone, R. W. Epigenetics in Cancer: Targeting Chromatin Modifications. *Mol. Cancer Ther.* **2009**, *8*, 1409−1420.

(2) Rodriguez-Paredes, M.; Esteller, M. Cancer Epigenetics Reaches Mainstream Oncology. *Nat. Med.* **2011**, *17*, 330−339.

(3) Robertson, K. D. DNA Methylation and Human Disease. *Nat. Rev. Genet.* **2005**, *6*, 597−610.

(4) Cottrell, S. E. Molecular Diagnostic Applications of DNA Methylation Technology. *Clin. Biochem.* **2004**, *37*, 595−604.

(5) Wee, E. J.; Rauf, S.; Shiddiky, M. J. A.; Dobrovic, A.; Trau, M. DNA Ligase-Based Strategy for Quantifying Heterogeneous DNA Methylation without Sequencing. *Clin. Chem.* **2015**, *61*, 163−171.

(6) Bhattacharjee, R.; Moriam, S.; Umer, M.; Nguyen, N. T.; Shiddiky, M. J. A. DNA Methylation Detection: Recent Developments in Bisulfite Free Electrochemical and Optical Approaches. *Analyst* **2018**, *143*, 4802−4818.

(7) Carrascosa, L. G.; Sina, A. A. I.; Palanisamy, R.; Sepulveda, B.; Otte, M. A.; Rauf, S.; Shiddiky, M. J. A.; Trau, M. Molecular Inversion Probe-Based SPR Biosensing for Specific, Label-Free and Real-Time Detection of Regional DNA Methylation. *Chem. Commun.* **2014**, *50*, 3585−3588.

(8) Heller, G.; Topakian, T.; Altenberger, C.; Cerny-Reiterer, S.; Herndlhofer, S.; Ziegler, B.; Datlinger, P.; Byrgazov, K.; Bock, C.; Mannhalter, C.; Hormann, G.; Sperr, W. R.; Lion, T.; Zielinski, C. C.; Valent, P.; Zochbauer-Muller, S. Next-Generation Sequencing Identifies Major DNA Methylation Changes during Progression of Ph + Chronic Myeloid Leukemia. *Leukemia* **2016**, *30*, 1861−1868.

(9) Cheow, L. F.; Quake, S. R.; Burkholder, W. F.; Messerschmidt, D. M. Multiplexed Locus-Specific Analysis of DNA Methylation in Single Cells. *Nat. Protoc.* **2015**, *10*, 619−631.

(10) Ehrlich, M.; Gama-Sosa, M. A.; Huang, L. H.; Midgett, R. M.; Kuo, K. C.; McCune, R. A.; Gehrke, C. Amount and Distribution of 5-Methylcytosine in Human DNA from Different Types of Tissues of Cells. *Nucleic Acids Res.* **1982**, *10*, 2709−2721.

(11) Sina, A. A. I.; Carrascosa, L. G.; Palanisamy, R.; Rauf, S.; Shiddiky, M. J. A.; Trau, M. Methylsorb: A Simple Method for Quantifying DNA Methylation using DNA-Gold Affinity Interactions. *Anal. Chem.* **2014**, *86*, 10179−10185.

(12) Sage, A. T.; Besant, J. D.; Lam, B.; Sargent, E. H.; Kelley, S. O. Ultrasensitive Electrochemical Biomolecular Detection Using Nanostructured Microelectrodes. *Acc. Chem. Res.* **2014**, *47*, 2417−2425.

(13) Jing, X.; Cao, X.; Wang, L.; Lan, T.; Li, Y.; Xie, G. DNA-AuNPs Based Signal Amplification for Highly Sensitive Detection of DNA Methylation, Methyltransferase Activity and Inhibitor Screening. *Biosens. Bioelectron.* **2014**, *58*, 40−47.

DOI: 10.1021/acsami.8b20144
ACS Appl. Mater. Interfaces XXXX, XXX, XXX−XXX

(14) Ko, J. W.; Woo, J. M.; Jinhong, A.; Cheon, J. H.; Lim, J. H.; Kim, S. H.; Chun, H.; Kim, E.; Park, Y. J. Multi-Order Dynamic Range DNA Sensor Using a Gold Decorated SWCNT Random Network. *ACS Nano* **2011**, *5*, 4365−4372.
(15) Pei, H.; Zuo, X. L.; Pan, D.; Shi, J. Y.; Huang, Q.; Fan, C. H. Scaffolded Biosensors with Designed DNA Nanostructures. *NPG Asia Mater.* **2013**, *5*, No. e51.
(16) Peterson, A. W.; Heaton, R. J.; Georgiadis, R. M. The Effect of Surface Probe Density on DNA Hybridization. *Nucleic Acids Res.* **2001**, *29*, 5163−5168.
(17) Zeng, D.; Zhang, H.; Zhu, D.; Li, J.; San, L.; Wang, Z.; Wang, C.; Wang, Y.; Wang, L.; Zuo, X.; Mi, X. A Novel Ultrasensitive Electrochemical DNA Sensor Based on Double Tetrahedral Nanostructures. *Biosens. Bioelectron.* **2015**, *71*, 434−438.
(18) Ge, Z.; Lin, M.; Wang, P.; Pei, H.; Yan, J.; Shi, J.; Huang, Q.; He, D.; Fan, C.; Zuo, X. Hybridization Chain Reaction Amplification of MicroRNA Detection with a Tetrahedral DNA Nanostructure-Based Electrochemical Biosensor. *Anal. Chem.* **2014**, *86*, 2124−2130.
(19) Pei, H.; Lu, N.; Wen, Y.; Song, S.; Liu, Y.; Yan, H.; Fan, C. A DNA Nanostructure-Based Biomolecular Probe Carrier Platform for Electrochemical Biosensing. *Adv. Mater.* **2010**, *22*, 4754−4758.
(20) Goodman, R. P.; Berry, R. M.; Turberfield, A. J. The Single-Step Synthesis of a DNA Tetrahedron. *Chem. Commun.* **2004**, *12*, 1372−1373.
(21) Huang, R.; He, N.; Li, Z. Recent Progresses in DNA Nanostructure-Based Biosensors for Detection of Tumor Markers. *Biosens. Bioelectron.* **2018**, *109*, 27−34.
(22) Li, Z.; Su, W.; Liu, S.; Ding, X. An Electrochemical Biosensor Based on DNA Tetrahedron/Graphene Composite Film for Highly Sensitive Detection of NADH. *Biosens. Bioelectron.* **2015**, *69*, 287−293.
(23) Zhu, C.; Yang, G.; Li, H.; Du, D.; Lin, Y. Electrochemical Sensors and Biosensors Based on Nanomaterials and Nanostructures. *Anal. Chem.* **2015**, *87*, 230−249.
(24) Haque, M. H.; Gopalan, V.; Yadav, S.; Islam, M. N.; Eftekhari, E.; Li, Q.; Carrascosa, L. G.; Nguyen, N. T.; Lam, A. K.; Shiddiky, M. J. A. Detection of Regional DNA Methylation Using DNA-Graphene Affinity Interactions. *Biosens. Bioelectron.* **2017**, *87*, 615−621.
(25) Povedano, E.; Valverde, A.; Ruiz-Valdepeñas Montiel, V.; Pedrero, M.; Yáñez-Sedeño, P.; Barderas, R.; Segundo-Acosta, P. S.; Peláez-García, A.; Mendiola, M.; Hardisson, D.; Campuzano, S.; Pingarrón, J. M. Rapid Electrochemical Assessment of Tumor Suppressor Gene Methylations in Raw Human Serum, and Tumor Cells and Tissues Using Immuno-Magnetic Beads and Selective DNA Hybridization. *Angew. Chem., Int. Ed.* **2018**, *57*, 8194−8198.
(26) Povedano, E.; Ruiz-Valdepeñas Montiel, V.; Valverde, A.; Navarro-Villoslada, F.; Yáñez-Sedeño, P.; Pedrero, M.; Montero-Calle, A.; Barderas, R.; Peláez-García, A.; Mendiola, M.; Hardisson, D.; Feliú, J.; Camps, J.; Rodríguez-Tomàs, E.; Joven, J.; Arenas, M.; Campuzano, S.; Pingarrón, J. M. Versatile Electroanalytical Bioplatforms for Simultaneous Determination of Cancer-Related DNA 5-Methyl- and 5-Hydroxymethyl-Cytosines at Global and Gene-Specific Levels in Human Serum and Tissues. *ACS Sens.* **2018**, DOI: 10.1021/acssensors.8b01339.
(27) Mao, X.; Jiang, J.; Xu, X.; Chu, X.; Luo, Y.; Shen, G.; Yu, R. Enzymatic Amplification Detection of DNA Based on "Molecular Beacon" Biosensors. *Biosens. Bioelectron.* **2008**, *23*, 1555−1561.
(28) Povedano, E.; Vargas, E.; Montiel, V. R.; Torrente-Rodriguez, R. M.; Pedrero, M.; Barderas, R.; Segundo-Acosta, P. S.; Pelaez-Garcia, A.; Mendiola, M.; Hardisson, D.; Campuzano, S.; Pingarron, J. M. Electrochemical Affinity Biosensors for Fast Detection of Gene-Specific Methylations with no Need for Bisulfite and Amplification Treatments. *Sci. Rep.* **2018**, *8*, No. 6418.
(29) Wee, E. J.; Shiddiky, M. J. A.; Brown, M. A.; Trau, M. eLCR: Electrochemical Detection of Single DNA Base Changes via Ligase Chain Reaction. *Chem. Commun.* **2012**, *48*, 12014−12016.
(30) Wee, E. J.; Rauf, S.; Koo, K. M.; Shiddiky, M. J. A.; Trau, M. μ-eLCR: a Microfabricated Device for Electrochemical Detection of DNA Base Changes in Breast Cancer Cell Lines. *Lab Chip* **2013**, *13*, 4385−4391.
(31) Dirks, R. M.; Pierce, N. A. Triggered Amplification by Hybridization Chain Reaction. *Proc. Natl. Acad. Sci. U.S.A.* **2004**, *101*, 15275−15278.
(32) Krejcova, L.; Richtera, L.; Hynek, D.; Labuda, J.; Adam, V. Current Trends in Electrochemical Sensing and Biosensing of DNA Methylation. *Biosens. Bioelectron.* **2017**, *97*, 384−399.
(33) Sina, A. A. I.; Howell, S.; Carrascosa, L. G.; Rauf, S.; Shiddiky, M. J. A.; Trau, M. eMethylsorb: Electrochemical Quantification of DNA Methylation at CpG Resolution Using DNA-Gold Affinity Interactions. *Chem. Commun.* **2014**, *50*, 13153−13156.
(34) Koo, K. M.; Wee, E. J.; Rauf, S.; Shiddiky, M. J. A.; Trau, M. Microdevices for Detecting Locus-Specific DNA Methylation at CpG Resolution. *Biosens. Bioelectron.* **2014**, *56*, 278−285.
(35) Koo, K. M.; Sina, A. A. I.; Carrascosa, L. G.; Shiddiky, M. J. A.; Trau, M. eMethylsorb: Rapid Quantification of DNA Methylation in Cancer Cells on Screen-Printed Gold Electrodes. *Analyst* **2014**, *139*, 6178−6184.
(36) Frommer, M.; McDonald, L. E.; Millar, D. S.; Collis, C. M.; Watt, F.; Grigg, G. W.; Molloy, P. L.; Paul, C. L. A Genomic Sequencing Protocol that Yields a Positive Display of 5-Methylcytosine Residues in Individual DNA Strands. *Proc. Natl. Acad. Sci. U.S.A.* **1992**, *89*, 1827−1831.
(37) Haque, M. H.; Bhattacharjee, R.; Islam, M. N.; Gopalan, V.; Nguyen, N. T.; Lam, A. K.; Shiddiky, M. J. A. Colorimetric and Electrochemical Quantification of Global DNA Methylation Using a Methyl Cytosine-Specific Antibody. *Analyst* **2017**, *142*, 1900−1908.
(38) Zhang, L.; Wei, M.; Gao, C.; Wei, W.; Zhang, Y.; Liu, S. Label-free Electrochemical Detection of Methyltransferase Activity and Inhibitor Screening Based on Endonuclease *Hpa*II and the Deposition of Polyaniline. *Biosens. Bioelectron.* **2015**, *73*, 188−194.
(39) He, X.; Su, J.; Wang, Y.; Wang, K.; Ni, X.; Chen, Z. A Sensitive Signal-On Electrochemical Assay for MTase Activity Using AuNPs Amplification. *Biosens. Bioelectron.* **2011**, *28*, 298−303.
(40) Lin, M.; Wen, Y.; Li, L.; Pei, H.; Liu, G.; Song, H.; Zuo, X.; Fan, C.; Huang, Q. Target-responsive, DNA Nanostructure-based E-DNA Sensor for MicroRNA Analysis. *Anal. Chem.* **2014**, *86*, 2285−2288.
(41) Bonnet, G.; Tyagi, S.; Libchaber, A.; Kramer, F. R. Thermodynamic Basis of the Enhanced Specificity of Structured DNA Probes. *Proc. Natl. Acad. Sci. U.S.A.* **1999**, *96*, 6171−6176.
(42) Wang, M.; Xu, Z.; Chen, L.; Yin, H.; Ai, S. Electrochemical Immunosensing Platform for DNA Methyltransferase Activity Analysis and Inhibitor Screening. *Anal. Chem.* **2012**, *84*, 9072−9078.
(43) Lin, M.; Wang, J.; Zhou, G.; Wang, J.; Wu, N.; Lu, J.; Gao, J.; Chen, X.; Shi, J.; Zuo, X.; Fan, C. Programmable Engineering of a Biosensing Interface with Tetrahedral DNA Nanostructures for Ultrasensitive DNA Detection. *Angew. Chem., Int. Ed.* **2015**, *54*, 2151−2155.
(44) Liu, S.; Su, W.; Li, Z.; Ding, X. Electrochemical Detection of Lung Cancer Specific MicroRNAs Using 3D DNA Origami Nanostructures. *Biosens. Bioelectron.* **2015**, *71*, 57−61.
(45) Yin, H.; Sun, B.; Zhou, Y.; Wang, M.; Xu, Z.; Fu, Z.; Ai, S. A New Strategy for Methylated DNA Detection Based on Photoelectrochemical Immunosensor Using Bi_2S_3 Nanorods, Methyl Bonding Domain Protein and Anti-his Tag Antibody. *Biosens. Bioelectron.* **2014**, *51*, 103−108.
(46) Liu, H.; Luo, J.; Fang, L.; Huang, H.; Deng, J.; Huang, J.; Zhang, S.; Li, Y.; Zheng, J. An Electrochemical Strategy with Tetrahedron Rolling Circle Amplification for Ultrasensitive Detection of DNA Methylation. *Biosens. Bioelectron.* **2018**, *121*, 47−53.
(47) Daneshpour, M.; Syedmoradi, L.; Izadi, P.; Omidfar, K. Femtomolar Level Detection of RASSF1A Tumor Suppressor Gene Methylation by Electrochemical Nano-Genosensor based on Fe_3O_4/TMC/Au Nanocomposite and PT-modified Electrode. *Biosens. Bioelectron.* **2016**, *77*, 1095−1103.
(48) Wang, L.; Yu, F.; Wang, F.; Chen, Z. Electrochemical Detection of DNA Methylation Using a Glassy Carbon Electrode Modified with a Composite Made from Carbon Nanotubes and β-Cyclodextrin. *J. Solid State Electrochem.* **2016**, *20*, 1263−1270.

DOI: 10.1021/acsami.8b20144
ACS Appl. Mater. Interfaces XXXX, XXX, XXX−XXX